Measurement of the lifetime of the $2\,^3P_2$ state in heliumlike krypton using a two-foil target

S. Cheng,* H. G. Berry, R. W. Dunford, D. S. Gemmell, E. P. Kanter, C. Kurtz, K. E. Rehm, and B. J. Zabransky
Physics Division, Argonne National Laboratory, Argonne, Illinois 60439
(Received 15 April 1994)

The lifetime of the $2\,^3P_2$ level in heliumlike krypton has been measured by an alternative method involving the use of a two-foil target. The experiment demonstrates the potential of this method which allows the standard beam-foil time-of-flight technique to be extended to shorter lifetimes. We measured a lifetime of 9.5 ± 0.9 ps, which is in reasonable agreement with current theoretical calculations.

PACS number(s): 32.70.Fw, 31.30.Jv, 31.10.+z

I. INTRODUCTION

The current goal in the study of the structure of highly charged ions is to fully understand the regime where both relativistic corrections and electron-electron correlations are simultaneously important. The ideal cases for such studies are high-Z two-electron ions. Two-electron ions are the simplest systems involving electron-electron correlations and relativistic effects become increasingly important at high Z. Measurements of lifetimes and transition energies are needed. Transition-energy measurements test calculations of binding energies while lifetime measurements test our understanding of the wave functions.

In this paper we report a measurement of the lifetime of the $2\,^3P_2$ level in heliumlike krypton. This state has a theoretical lifetime [1] of 9.5 ps, which corresponds to a decay length of only 380 μm at a typical ion-beam velocity of $0.1c$. This short decay length poses problems for the standard beam-foil time-of-flight technique in which a decay curve is obtained by moving an exciter foil relative to the field of view of a photon detector. The method becomes difficult as the decay length becomes shorter than about 1 mm because one must collimate the detector so that it can view the region close to the foil without viewing the foil itself. To avoid this problem in our measurement, we employed a two-foil target in a modification of the traditional beam-foil time-of-flight technique. Our method has the potential for extending measurements to much shorter decay lengths than have been practical in the past. This is important for the study of higher-Z ions since lifetimes get shorter as Z increases.

Figure 1 shows the low-lying energy levels of heliumlike krypton, including the theoretical lifetimes. An interesting feature of these energy levels is the wide range of lifetimes extending from 0.66 fs for the $2\,^1P_1$ level to 1.4 ns for the $2\,^3P_0$ level. The $2\,^3P_2$ level decays 90% of the time by $M2$ emission to the ground state [1]. This is an interesting case since $M2$ decays are rare in atomic physics. At low Z, the $2\,^3P_2$ level decays mostly by an electric dipole transition to the $2\,^3S_1$ level. Above $Z=17$, the magnetic quadrupole transition to the ground state dominates. The $M2$ transition probability increases as Z^8 while the $E1$ transition probability increases only linearly with Z [2]. Nonrelativistic calculations of the $M2$ decay rate have been made by Mizushima [3], Garstang [4,5], Drake [6,7], and Jacobs [8]. Relativistic corrections have been calculated by Gould, Marrus, and Mohr [9] and Johnson and co-workers [10,11,1]. The latter used the relativistic-random-phase approximation (RRPA) to determine both the $M2$ and the $E1$ transition probabilities. The RRPA results for He-like krypton are

$$\omega_{\rm rel}^{2\,^3P_2\ M2}=9.43\times10^{10}\ {\rm s}^{-1}\ , \quad (1)$$

$$\omega_{\rm rel}^{2\,^3P_2\ E1}=1.08\times10^{10}\ {\rm s}^{-1}\ , \quad (2)$$

corresponding to a lifetime

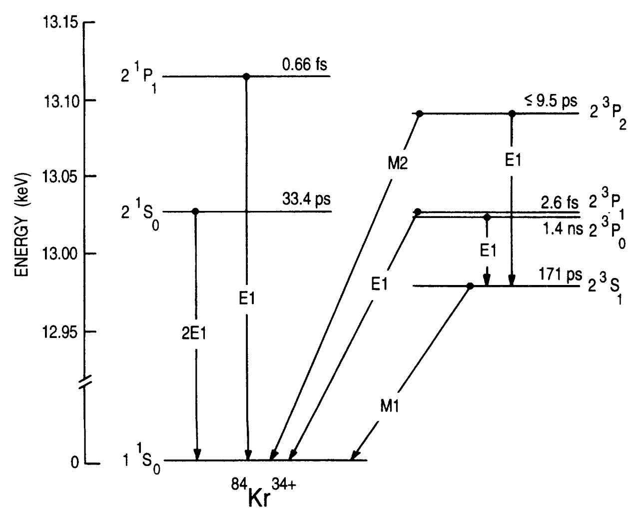

FIG. 1. Low-lying energy levels for heliumlike krypton including theoretical lifetimes and decay modes.

*Present address: Department of Physics and Astronomy, University of Toledo, Toledo, OH 43606.

$$\tau_{\rm rel}^{2\,^3P_1}=9.52 \text{ ps} . \quad (3)$$

The branching ratio for the $M2$ decay is

$$b_{\rm rel}^{2\,^3P_2}=\frac{\omega_{\rm rel}^{2\,^3P_2\,M2}}{\omega_{\rm rel}^{2\,^3P_2\,E1}+\omega_{\rm rel}^{2\,^3P_2\,M2}}=0.897 . \quad (4)$$

Subsequent experimental work has resulted in measurements of the decay rate at values of Z ranging from 9 to 47. A review of the results prior to 1978 has been given by Marrus and Mohr [2]. The emphasis recently has been on improved precision for high-Z ions.

II. EXPERIMENT

The ^{84}Kr ions used in this measurement were accelerated at the superconducting accelerator ATLAS to a final energy of 700 MeV and passed through a 200-μg/cm^2 carbon foil where about 35% emerged in the 34+ charge state. The beam velocity was measured to 0.1% using a resonant time-of-flight energy measurement system [12]. This system is located upstream of the 200-μg/cm^2 stripper foil, so that energy loss corrections for this foil and the target foil had to be applied. This was done using standard tables for the energy loss of ions traversing solids [13]. The error in the velocity determination was about 0.5%, dominated by the uncertainty in the thickness of the stripper foil.

The target consisted of two thin carbon foils which were moved relative to each other using a translation stage which could be positioned to a precision of $\frac{1}{3}$ of a micrometer. A beam of 700-MeV He-like Kr^{34+} ions was incident on the first foil. The beam emerging from this foil contained various charge states in various states of electronic excitation. Ions that emerged from the first foil in the (heliumlike) $2\,^3P_2$ state, entered the second foil in either the $2\,^3P_2$ state or in the heliumlike ground state (or the $2\,^3S_1$ state) depending upon whether the ion decayed in the region between the foils. The distribution of charge states and electronic states downstream of the second foil depended on the state of the ions entering this foil. When the foil separation was increased, the fraction of the beam that entered the second foil in the $2\,^3P_2$ state decreased, thus changing the composition of states in the beam downstream of the target. We used x-ray spectroscopy to study this excited state composition as a function of foil separation and to deduce the lifetime of the heliumlike $2\,^3P_2$ state.

We also studied the feasibility of an alternate form of the two-foil lifetime experiment which involved measuring the charge-state fraction downstream of the second foil with a magnetic spectrograph. In this case, if an ion emerges from the first foil in the $2\,^3P_2$ state but decays to the ground state before reaching the second foil, it tends to capture an electron in the second foil to produce a lower charge state. For example, we found that for heliumlike krypton ions incident on a 20-μg/cm^2 foil, only 2% are stripped to a higher charge state while 64% emerge in a lower charge state. On the other hand, if the ion remains in the $2\,^3P_2$ state, it has a much higher probability for being stripped to the hydrogenlike charge state. As the separation between the foils is increased, fewer ions are in the excited state and so the H-like fraction in the beam emerging from the second foil decreases. The lifetime could then be determined by measuring the charge state as a function of the foil separation.

The charge-state fractions downstream of the target were studied using an Enge split-pole spectrograph with a position-sensitive parallel-plate avalanche detector in the focal plane. We studied the changes in these charge-state distributions as a function of foil separation, varying the target materials and thicknesses of the two foils. As expected, the data show that the charge-state distribution shifts towards the lower charge states as the foils are separated. We plan to exploit this effect in future lifetime experiments.

A simplified schematic of the apparatus for the x-ray form of the experiment is given in Fig. 2. A Si(Li) x-ray detector located downstream of the target is collimated so that it views a region from 5 to 10 mm downstream of the fixed foil of the two foil target. The foil separation is changed by moving the first foil, so the distance between the second foil and the region along the beam being viewed by the Si(Li) detector remains fixed.

In Fig. 3 we show a plot of the fraction of excited ions emerging from the second foil that survive to a given distance from the foil. This shows that the $2\,^3P_2$ state ions decay before reaching the region being viewed by the detector, but that a large fraction of $2\,^3S_1$ ions survive and a substantial fraction decay in view of the detector.

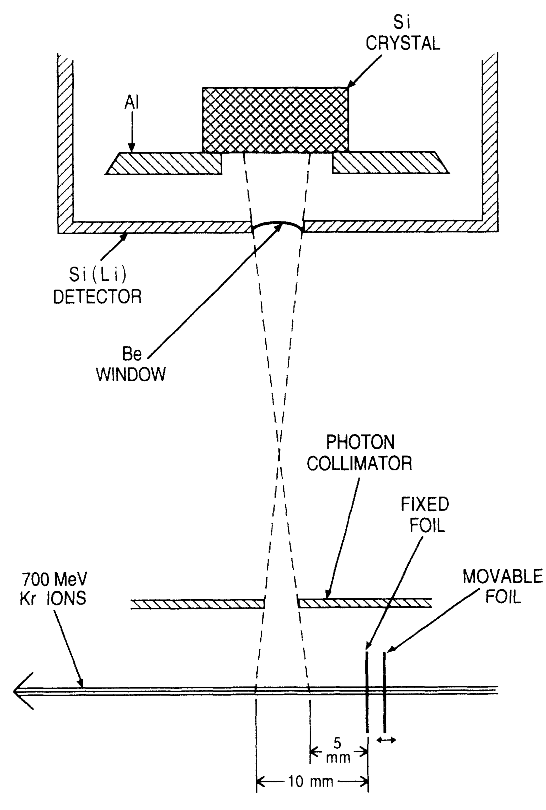

FIG. 2. Schematic diagram of the x-ray form of the two-foil lifetime experiment.

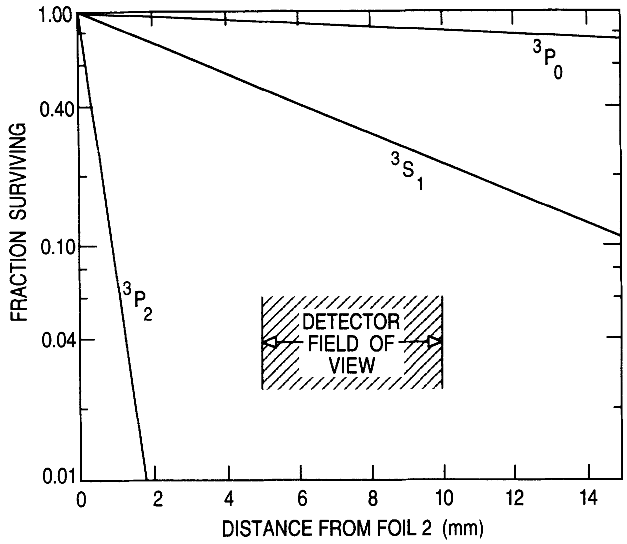

FIG. 3. Fraction of ions in various states which survive to a given distance from the second foil.

Almost all the ions in the $2\,^3P_0$ state survive to the detector, but only a small fraction decay within view of the detector. So the $2\,^3S_1$ state is the main source for $n=2\rightarrow1$ x-rays from He-like Kr incident on the detector.

III. RESULTS

Figure 4 shows the 13-keV line seen in the Si(Li) detector for two different foil positions. Each line corresponds to the same integrated beam current so the change in intensity as the foils are separated is evident. In the chosen configuration this line is predominantly from decay of the $2\,^3S_1$ level. For each foil position we fit the line to a Gaussian and a quadratic background. These data corrected for dead time and pileup are shown in Fig. 5 as a function of the separation between the two foils for the case of a 100-μg/cm^2 carbon foil followed by a 20-μg/cm^2 carbon foil. The changes in intensity correspond to the decay of excited states in the region between the foils. Although there is a large constant offset from $2\,^3S_1$ states made at the second foil, the foil-separation-dependent part is significant. The intensity at small foil separation has a 25% contribution associated with the intensity of the $2\,^3P_2$ and $2\,^3S_1$ states existing between the two foils. The solid line in Fig. 5 is a fit to the data using two exponentials and a constant background. The value of the $2\,^3S_1$ lifetime was kept fixed since it was measured in an earlier experiment [14,15]. In the inset, we show a logarithmic plot of the fit to the region at small foil separation after subtracting the $2\,^3S_1$ contribution. From these data we determine the lifetime of the $2\,^3P_2$ state to be 9.5 ± 0.9 ps, where the error is due entirely to the statistical uncertainty (2 h integration). Various systematic errors were considered including cascades from higher excited states, but these were found to be negligible at the present level of precision.

In Fig. 6 we compare the most precise experimental results for $M2$ transition probabilities with theory. The experimental values are obtained by subtracting the theoretical $E1$ transition probabilities [1] from the experimental results. The dashed line shows the nonrelativistic calculation. It can be seen from this plot that a more precise experimental result for ions in the $Z=30-40$ region is needed in order to better characterize the Z dependence of the lifetime of the $2\,^3P_2$ state in heliumlike ions and to provide a test of the relativistic corrections.

An interesting question raised by our data concerns the

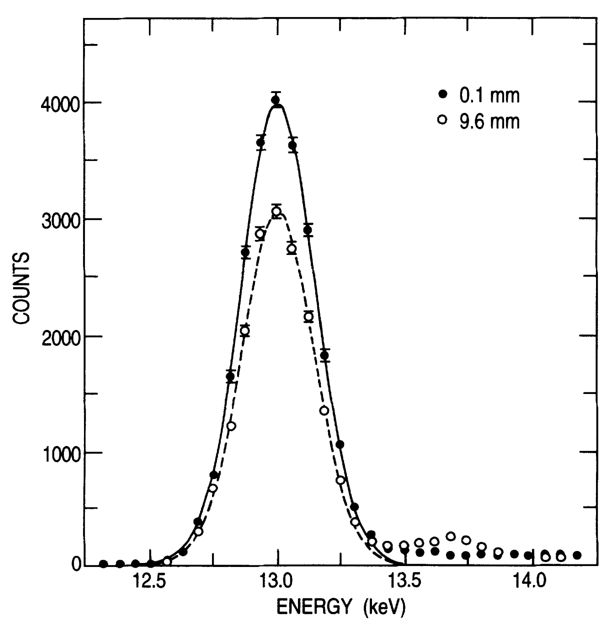

FIG. 4. Line at 13 keV seen in the Si(Li) detector for two different foil separations.

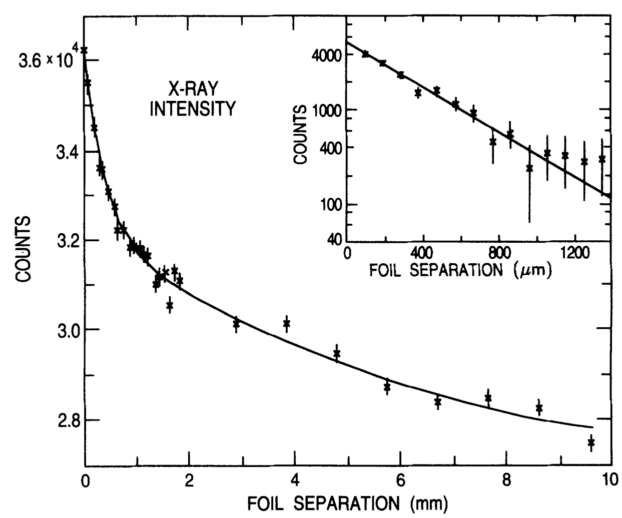

FIG. 5. Intensity of the $M1$ line in the x-ray detector as a function of the separation between the foils in the two-foil target. The solid line is a fit with two A_{M2}^{theor} exponentials and a constant background. The inset is a plot of the decay curve after subtraction of the constant background and the $2\,^3S_1$ component.

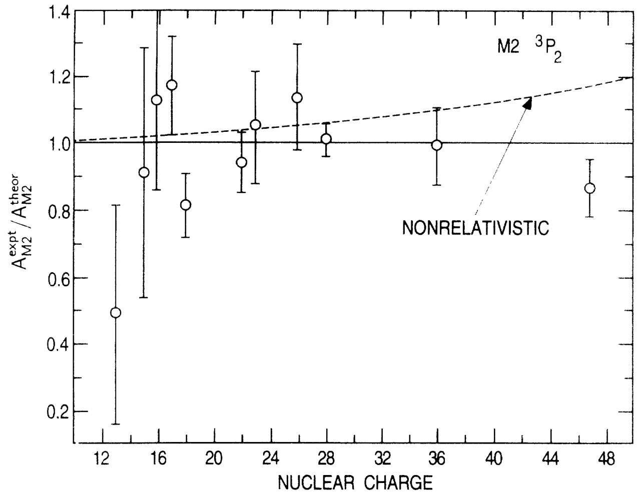

FIG. 6. Comparison of theory $A_{M2}^{\rm theor}$ [1] and experiment $A_{M2}^{\rm expt}$ for the $M2$ transition probability for the $2\,^3P_2$ level. The dashed line is the prediction of the nonrelativistic theory [6]. The experimental results are obtained by subtracting the theoretical values for the $E1$ transition from the experimental determinations of the total transition probability. References to experimental values $Z=13$ [23]; 15 [24]; 16 [25]; 17 [26]; 18 and 22 [27]; 23 and 26 [9]; 28 [28]; 36 this work; 47 [29].

mechanism for the conversion of excited ions entering the second foil to ions in the $2\,^3S_1$ level exiting from this foil. We will only comment briefly on this question here. Consider the case of an ion in the heliumlike $1s2p\,^3P_2$ state which enters the thin (20-μg/cm^2) second foil. In the following, we list four possibilities for the mechanism for conversion of this ion to a $2\,^3S_1$-state ion in the region downstream of the second foil.

(a) The $2\,^3S_1$ state could be populated by multiple collisions in the foil, e.g., stripping of the $2\,^3P_2$ state to the Kr^{35+} ground state followed by electron capture to the He-like $2\,^3S_1$ level. Such processes have low probability in the thin 20-μg/cm^2 second foil. For example, the mean free path for stripping an ion in the $2\,^3P_2$ state in C is about 5 times the thickness of a 20-μg/cm^2 foil and the probability that a Kr^{35+} ground-state ion will capture to the He-like $2\,^3S_1$ state in the 20-μg/cm^2 foil is less than 1%.

(b) The $2\,^3P_2$ state has a branch to the $2\,^3S_1$ state via an $E1$ transition (see Fig. 1). This will increase the population of the $2\,^3S_1$ level and to the extent that this state survives the second foil, we have a possible foil-separation-dependent $2\,^3S_1$ state population downbeam of the second foil. (Note: there is a subtle point here. The net effect depends on the relative survival probability of the two states in the second foil. For example, in the limit of a very thin foil, in which both the $2\,^3P_2$ and $2\,^3S_1$ states survive the foil with high probability, there is no foil-dependent effect since a constant 10% of the $2\,^3P_2$ states created in the first foil will end up in the $2\,^3S_1$ state.) We have modeled the cascade effect and find that it gives rise to a small increase in the $2\,^3S_1$ population as a function of foil separation, but this effect is small compared to the effect we observe in the experiment.

(c) The $2\,^3P_2$ and $2\,^3S_1$ levels can be mixed by the wake field within the foil [16–20] resulting in a coherent superposition with an amplitude which oscillates in time within the foil. The amplitude for an ion which enters the foil in the $2\,^3P_2$ state to be in the $2\,^3S_1$ state at the foil exit will depend on the thickness of the foil. The wake field for a 700-MeV Kr ion in a carbon foil is about 2×10^9 V/cm [16,21]. In this field the $2\,^3S_1-2\,^3P_2$ mixing is only about 6×10^{-3} and so this process is expected to be too small to explain our result.

(d) Individual collisions with foil atoms can give rise to intrashell transitions between the triplet-s and triplet-p levels. We estimated the cross sections for such $2s$-$2p$ transitions using a calculation of McGuire *et al.* [22] and found the cross section to be about 4×10^{-18} cm^2 for He-like Kr ions incident on a carbon foil. This gives a mean free path of 5 μg/cm^2, which indicates that this is an important effect. On average, several excitation events would be expected in traversing the foil so that one can consider the triplet-s and triplet-p states to be completely mixed within the foil. This seems to be the most likely mechanism for the effect observed in this experiment.

As a check, we developed a simple model to track the evolution of charge states and electronic excitations as the ions traverse the two-foil target. The model considers four charge states: (a) bare, (b) one electron, (c) two electrons, and (d) three or more electrons. The one- and two-electron species are further broken down into their ground electronic states and the various possible $n=2$ excited states. We solve numerically for the populations of each these states as the ions propagate through the first foil, the vacuum, and then the second foil. We use estimates of cross sections for capture, loss, excitation, and deexcitation of electrons as well as theoretical lifetimes for decay in vacuum. We also account for the lifetimes within the foils which are in general quite different because of the strong perturbations existing in the foils. The results from this model further confirm our conclusion that intrashell mixing is the dominant mechanism for conversion of ions in the $2\,^3P_2$ state to ions in the $2\,^3S_1$ state within the foil.

IV. CONCLUSION

In conclusion, we have demonstrated an alternative method for measuring lifetimes in highly charged ions and used it to obtain a measurement of the lifetime of the $2\,^3P_2$ state in He-like Kr. The full power of the method is that it is extensible to measurements of lifetimes much shorter than 1 ps. The two-foil target also provides a unique way to study the beam-foil interaction. In particular, it provides a means for studying what happens to specific excited states interacting with the foil. The different states are identified by their characteristic change in population as a function of foil separation.

ACKNOWLEDGMENTS

We are indebted to the ATLAS staff for excellent technical assistance during this experiment. We also thank Heidi Reichenbach for help with data analysis. This work was supported by the U.S. Department of Energy, Office of Basic Energy Sciences under Contract No. W-31-109-ENG-38.

[1] C. D. Lin, W. R. Johnson, and A. Dalgarno, Phys. Rev. A **15**, 154 (1977).
[2] R. Marrus and P. J. Mohr, Adv. At. Mol. Phys. **14**, 181 (1978).
[3] M. Mizushima, J. Phys. Soc. Jpn. **21**, 2335 (1966).
[4] R. H. Garstang, Astrophys. J. **148**, 579 (1967).
[5] R. H. Garstang, Publ. Astron. Soc. Pac. **81**, 488 (1969).
[6] G. W. F. Drake, Astrophys. J. **158**, 1199 (1969).
[7] G. W. F. Drake, Astrophys. J. **163**, 439 (1971).
[8] V. L. Jacobs, J. Phys. B **5**, 213 (1972).
[9] H. Gould, R. Marrus, and P. J. Mohr, Phys. Rev. Lett. **33**, 676 (1974).
[10] W. R. Johnson and C. D. Lin, Phys. Rev. A **14**, 565 (1976).
[11] W. R. Johnson, C. D. Lin, and A. Dalgarno, J. Phys. B **9**, L303 (1976).
[12] R. Pardo, B. E. Clifft, P. Denhartog, D. Kovar, W. Kutschera, and K. E. Rehm, Nucl. Instrum. Methods A **270**, 226 (1988).
[13] J. F. Ziegler, *Handbook of Stopping Cross Sections for Energetic Ions in all Elements* (Pergamon, New York, 1980).
[14] R. W. Dunford, D. A. Church, C. J. Liu, H. G. Berry, M. L. A. Raphaelian, M. Hass, and L. J. Curtis, Phys. Rev. A **41**, 4109 (1990).
[15] S. Cheng, R. W. Dunford, E. P. Kanter, H. G. Berry, L. J. Curtis, and A. E. Livingston, Bull. Am. Phys. Soc. **37**, 1147 (1992).
[16] N. Bohr, K. Dan. Vidensk. Selsk. Mat.-Fys. Medd. **18**, No. 8 (1948).
[17] A. Faibis, R. Kaim, I. Plesser, and Z. Vager, Nucl. Instrum. Methods **170**, 99 (1980).
[18] D. Gemmell and Z. Vager, in *Treatise on Heavy-Ion Science*, edited by D. A. Bromley (Plenum, New York, 1985), Vol. 6.
[19] J. Müller and J. Burgdörfer, Phys. Rev. A **43**, 6027 (1991).
[20] J. Burgdörfer, Nucl. Instrum. Methods B **67**, 1 (1992).
[21] L. C. Northcliffe and R. F. Schilling, Nucl. Data Tables A **7**, 233 (1970).
[22] J. H. McGuire, D. J. Land, J. G. Brennan, and G. Basbas, Phys. Rev. A **19**, 2180 (1979).
[23] B. Denne, S. Huldt, J. Pihl, and R. Hallin, Phys. Scr. **22**, 45 (1980).
[24] A. E. Livingston and S. J. Hinterlong, Nucl. Instrum. Methods **202**, 103 (1982).
[25] C. L. Cocke, B. Curnutte, and R. Randall, Phys. Rev. A **9**, 1823 (1974).
[26] C. L. Cocke, B. Curnutte, J. R. Macdonald, and R. Randall, Phys. Rev. A **9**, 57 (1974).
[27] W. A. Davis and R. Marrus, Phys. Rev. A **15**, 1963 (1977).
[28] R. W. Dunford, C. J. Liu, J. Last, N. Berrah-Mansour, R. Vondrasek, D. A. Church, and L. J. Curtis, Phys. Rev. A **44**, 764 (1991).
[29] A. Simionovici, B. B. Birkett, J. P. Briand, P. Charles, D. D. Dietrich, K. Finlayson, P. Indelicato, D. Liesen, and R. Marrus, Phys. Rev. A **48**, 1695 (1993).